Desalination 404 (2017) 215–223

Contents lists available at ScienceDirect

Desalination

journal homepage: www.elsevier.com/locate/desal

Effect of boron rejection and recovery rate on a single-pass design of SWRO using hybrid membrane inter-stage design (HID) concept

Doseon Han, Moonhyun Hwang, In S. Kim *

Global Desalination Research Center (GDRC), School of Earth Sciences and Environmental Engineering, Gwangju Institute of Science and Technology (GIST), 123 Cheomdangwagi-ro, Buk-gu, Gwangju 61005, Republic of Korea

HIGHLIGHTS

- The performance of pressure vessel could be optimized with applying HID.
- The most influenced design factor on boron rejection was feed water temperature.
- The design using high flux membranes on tail position is preferred since it doesn't exceed recovery rate limit.
- Application of HID can save up to 0.41 kWh/m^3 of SEC on SWRO process.

ARTICLE INFO

Article history:
Received 23 May 2016
Received in revised form 13 September 2016
Accepted 5 November 2016
Available online 18 November 2016

ABSTRACT

Seawater reverse osmosis (SWRO) has been applied as a desalination method to provide potable water to regions under the stress of water shortages and is more effective than other desalination processes. However, specific energy consumption (SEC) must be considered in SWRO process design because of its energy intensive features. Hybrid membrane inter-stage design (HID) was examined to enhance the SEC efficiency of the reverse osmosis process. The additional removal of boron may improve the water quality by adding a second pass. However, this additional factor may increase costs. This study investigated a potential HID that satisfies water quality standards with single pass SWRO only. The element configuration for the HID was evaluated by changes in SEC, salt rejection, and boron rejection under general seawater quality conditions. Case studies were also conducted to estimate the energy efficiency of the HID under three feed conditions: high concentration and high temperature (Case 1); low concentration and high temperature (Case 2); and low concentration and low temperature (Case 3). The results showed HID application can save up to 0.41 kWh/m^3 of SEC. Temperature is a more important design factor than recovery rate for HID application.

1. Introduction

Reverse osmosis (RO) technology has recently dominated the desalination market because it has the least expensive unit cost for the production of water [1,2]. Despite the low unit cost, RO technology involves a more energy intensive process for the treatment of seawater or saline water than other conventional fresh water resources [3,4]. Accordingly, the main purpose of seawater reverse osmosis (SWRO) research is the reduction of energy consumption. Major improvements in SWRO energy efficiency over the last few decades have included the development of thin-film composite membranes and energy recovery devices [2,5–10]. In addition, SWRO system design improvements from a membrane module to an RO train have further enhanced SWRO energy efficiency [11–14]. The RO module configuration in pressure vessels (PVs) has been a focus of SWRO design research recently. It is common for the flux of the first element position to be relatively higher than the tail side position elements in a SWRO PV because of the higher osmotic pressure at the tail position element from the gradual recovery of feed water. An internally staged design (ISD) concept was developed as a novel RO module configuration in a PV by Dow Chemical (PCT/US05/06224) to solve these unbalanced flux problems [15]. Two or more membrane types were used in the same PV for the ISD, in which higher productivity membranes were located in other positions than the first and second position. This ISD not only enhanced total productivity of the PV unit but also reduced the fouling potential of the front position elements. Molina et al. showed the cost saving by retrofitting the conventional pressure vessel design to ISD with fouling factors and feed temperature changes. However, this study was conducted with 2nd pass SWRO process. It means that there were no concerns about permeate water quality due to the presence of 2nd pass [16–18].

The hybrid membrane inter-stage design (HID) uses commercial SWRO membranes from three different manufacturers. This concept

* Corresponding author.
E-mail address: iskim@gist.ac.kr (I.S. Kim).

http://dx.doi.org/10.1016/j.desal.2016.11.007
0011-9164/

has been used without limiting the element position and manufacturer. Penete et al. extended the ISD concept which applies only Dow Chemical membrane elements to the HID concept, applying membrane modules in every membrane manufacturer. They showed the performance comparison and retrofitting strategy for canary island SWRO plants. These two reports mentioned that ISD and HID can reduce total cost and energy consumptions. [19].

The RO process must be optimized according to diverse design factors such as feed water quality, operating conditions, regional drinking water standards, and plant management [20–26]. Boron is one of the key design factors in the SWRO process owing to its low removal rate compared with other ions. The average boron concentration in seawater is 4.8 mg/L, and it exists as boric acid and borate ions in seawater [27, 28]:

$$B(OH)_3 + H_2O \rightleftharpoons B(OH)_4^- + H^+, pK_a = 9.2 \text{ at pH 7 and 25 °C.}$$

Boric acid is a major component of the boron molecular form within a low pH range. Boric acid exists in an uncharged form in aqueous solution; thus, hydrated boron molecules are relatively lower than other ion species in seawater. Therefore, conventional SWRO membranes remove less boron (approximately 70%) than other anions and cations [29]. However, the borate ion form is completely hydrated and charged in feed solutions in a high pH range and causes a high rejection rate in the SWRO membrane process owing to size exclusion and repulsion phenomena. Although the World Health Organization revised the boron concentration limit to 2.4 mg/L in 2012 [30], the European Union maintains a boron limit of 1.0 mg/L for potable water [31] because of the risk it presents to crops [32–34]. Therefore, a process should be designed that results in boron concentrations of 1 mg/L or lower to provide seawater desalination to various countries.

High boron removal rates have been achieved mainly through the use of additional processes, ion exchange (IX), and a second pass with pH adjustment. These post-treatment processes incur additional capital and operating costs between 0.04 $/m^3 and 0.1 $/m^3 [29, 35]. Researchers have attempted to adjust boron levels with only a single pass and no post-treatment to avoid these additional costs. Their results indicated SWRO membrane boron removal ability was enhanced and satisfied the water quality criteria using single-pass SWRO systems with various operating conditions and membrane types. The pH control was the main issue for the single-pass SWRO system both with and without a chemical dosage because of the relationship between scaling problems and boron removal [36–39]. However, ISD research has not yet evaluated boron removal and has instead focused on energy efficiency through the application of high-flux membranes.

The main objective of this study is to develop novel approach of SWRO vessel design by using the HID on the optimal single-pass design and suitable operating conditions of commercial SWRO membranes to meet 1 mg B/L water with commercial membrane elements. Inter-staged technique was utilized not only to solve unbalanced flux distribution problem, the main focus of previous HID studies, but also to enhance the process performance. In this study, higher flux membrane element was located not only in the front position but also in the tail position to extend HID concept for optimizing SWRO vessel design. Performance of HID were evaluated by commercial SWRO system model tool provided by the manufacturer. Membrane configurations were evaluated by comparing three factors: permeate total dissolved solids (TDS), boron concentration, and the SEC on a single-pass SWRO system. Then, three case studies were conducted to estimate the energy efficiency of the HID under three feed conditions: high concentration and high temperature (Case 1), low concentration and high temperature (Case 2), and low concentration and low temperature (Case 3).

2. Materials and method

2.1. Pressure vessel design & operating condition

ROSA9, the commercial simulation program by Dow Water & Process Solutions, was used to evaluate HID performance. Computational assessment of membrane performance was performed on commercial 8-inch membranes made by Dow. ROSA9 provides the ISD analysis. Three types of RO membrane were selected based on their features: high-rejection membrane (SW30XHR-400i), standard membrane (SW30HRLE-400i), and high-flux membrane (SW30ULE-400i). The specifications of selected elements are in Table 1.

Table 2 shows the membrane configurations in the simulation. The PV composed of seven (3 + 4 element configuration) elements to estimate the boron removal ability of a single pass. The reason 3 + 4 configuration was chosen is that half of permeate was produced on front 3 position elements. So, permeate TDS concentration was controlled by each of membrane types respectively on 3 + 4 (element) design. Accordingly, 3 + 4 (element) design was used in this study. Single pass could consist of single stage or 2 stages, but there would be too many configurations of 2 stage array (e.g. 2:1; 3:2; 4:2, etc.). Recent commercial membrane performance has been rapidly improved, so sufficient recovery rates are obtained in the single stage. Also, single stage was used for the simple analysis of performance of HID.

Operating flow rate was set at 10 m^3/h, and pump efficiency was assumed to be 80%. Optimal recovery rates of each membrane configuration were calculated by comparing the SEC. Fig. 1 shows a schematic diagram of the 7-element PV design with the conventional design and the HID. The conventional design used one membrane type, and the HID used two membrane types in the PV. The front position was located in the direction of feed water inflow. The tail position was located in the direction of concentrated water emission.

2.2. Feed water quality

Feed quality in this study was separated according to two conditions, general feed condition and various real feed quality data. Three factors were used first to obtain general information regarding the performance of each membrane configuration PV design under general seawater feed condition: SEC, TDS, and boron concentration of permeate water. The analysis was conducted at a recovery rate of 45% at 20 °C. The feed water was assumed to flow into the SWRO PV after the conventional pre-treatment process (SDI < 5). The ionic composition of the feed water was referred to as the "seawater" composition reported by M. J. Atkinson et al. [40]. The feed TDS value was 35,000 mg salt/L; the boron concentration was 4.53 mg boron/L; and the pH was 8.2.

Three locations where the SWRO process is mainly used were selected to find the optimal PV design. Table 3 shows the feed water quality of the three target locations in the study (Case 1, Case 2, and Case 3). The feed seawater has a high temperature and high TDS value in Case 1, a low TDS and high temperature in Case 2, and a low temperature and general feed quality in Case 3. Although these three cases cannot

Table 1
Specifications of selected RO membranes (32,000 ppm NaCl, 800 psi, 25 °C).

Membrane	Flow (GPD (m^3/d))	Salt rejection (%)	Boron rejection (%)	Type
SW30XHR-400i	6000 (22.7)	99.82	93	High rejection
SW30HRLE-400i	7500 (28.4)	99.8	92	Standard
SW30ULE-400i	11,000 (41.6)	99.7	89	High flux

Table 2
Membrane configuration of conventional and HID PV designs.

Configuration	Membrane element
XHR	SW30XHR-400i
HRLE	SW30HRLE-400i
ULE	SW30ULE-400i
HID 1	(SW30XHR-400i) 3 + (SW30HRLE-400i) 4
HID 2	(SW30XHR-400i) 3 + (SW30ULE-400i) 4
HID 3	(SW30HRLE-400i) 3 + (SW30XHR-400i) 4
HID 4	(SW30HRLE-400i) 3 + (SW30ULE-400i) 4
HID 5	(SW30ULE-400i) 3 + (SW30XHR-400i) 4
HID 6	(SW30ULE-400i) 3 + (SW30HRLE-400i) 4

describe all possible feed qualities, we expect the advantages of HID can be estimated from these three cases results.

3. Results and discussion

3.1. Tradeoff relation of HID PV

Many different parameters such as the flow rate of feed, TDS rejection, operational pressure, flux, and fouling potential should be considered in an SWRO process design. The RO membrane performance was tested under standard conditions (20 °C, 32,000 mg/L). However, commercial SWRO plant designs operated with a PV unit containing six or more membrane elements evaluate performance not by each membrane element but for the overall PV unit. Although the RO membranes in this PV unit were developed for high permeate flux with high salt rejection for high efficiency, their performance is generally a tradeoff between salt rejection ability and water permeability. Therefore, the PV designs with one type of RO membrane must focus on either salt rejection or permeate flux. Conversely, both high rejection membranes and high permeate flux membranes are used in the HID; thus, the design range of the PV is more flexible. Fig. 2 shows the relationship between SEC and rejection of salt and boron. These data were obtained under one PV condition without an energy recovery device (ERD) to evaluate only the performance of the membrane configuration of a PV with an average flux of 17.3 LMH and total active area of 260.12 m^2.

Fig. 2 shows the performance and linear relationship in the PV, except for the XHR and HID 6 configurations. The highest salt and boron rejections are in the XHR (99.77% and 91%, respectively) configuration and the lowest rejections are in the ULE configuration (99.31% and 78%).

The HID 6 configuration has a slightly less than linear relationship owing to the high-flux membranes (SW30ULE-400i) in the front position of the PV. Despite the same front configuration, HID 5 has high SEC and rejection. Although HID 2 and HID 4 exhibit a similar relationship to HID 6 and HID 5, they have lower rejection rates for salt and boron than HID 5 and HID 6, respectively. This indicates that the module configuration of the tail position has more of an effect on water quality and the front membrane configuration in the PV has more of an impact on flux. Therefore, module configuration can be designed optionally to control water quality level or energy reduction depending on feed water quality. The two types of module configuration in the PV in this study were fixed to three versus four to recover 50% of the total flux by the front modules. However, if a three or more type module configuration is applied, this flexibility is expected to be superior.

Fig. 3 shows the design range in RO configuration under the conditions of 20 °C, salt 35,000 ppm, and 45% recovery rate to maintain water quality below the 1 mg/L boron concentration. Allowable boron concentration indicates the limit of feed boron concentration when designing an SWRO process for certain operating conditions. The difference of design capacity indicates the difference of allowable boron feed concentration among the pressure vessel designs. The difference of design capacity 1 is 2.96 B mg/L between XHR (11.05 B mg/L) and HRLE (8.09 B mg/L). The difference of design capacity 2 is 3.47 B mg/L between HRLE (8.09 B mg/L) and ULE (4.62 B mg/L). When we apply the HID concept, there are 8 different design capacities in between XHR and ULE. The difference of design capacity 1 can be composed of 3 different design capacities (XHR to HID3, HID3 to HID1 and HID1 to HRLE). Therefore, the differences of allowable feed boron concentration are decreased to 1.61 mg/L, 0.38 mg/L and 0.97 mg/L. As seen in Fig. 3, if the PV is designed with only one type of RO module, it may be inefficient and difficult to satisfy the required quality beyond its optimum feed boron concentration range. HID can effectively redeem this narrow the difference of design capacity by the relationship between rejection rate and SEC. Figs. 2 and 3 show that when the HID technique is applied to a SWRO PV design, a new HID can also be designed according to salt and boron rejection.

3.2. Symmetric HID design

There are symmetric designs among the HID pressure designs (i.e., HID 1 and HID 3, HID 2 and HID 5, and HID 4 and HID 6). Symmetric design refers to the same membrane configuration used in a different position. For example, HID 1 and HID 3 consist of the SW30XHR-400i (high rejection membrane) and SW30HRLE-400i (standard membrane) models. In the HID 1 design, the high rejection membrane was positioned on the front side of the vessel. However, high rejection membranes were positioned on the tail side of the vessel in the HID 2 design. All the symmetric designs show that HID 3, HID 5, and HID 6 possessing high-flux membranes on the front side have higher salt rejection rate and lower SEC (Fig. 2).

Fig. 4 shows the recovery rate of each element as a function of total recovery rate. The commercial membrane element has its own limit recovery rate (13%) and design flux. The limit recovery rates and maximum permeate flux are determined by the fouling tendency of feed seawater, which was Silt Density Index (SDI) value, used <5 (conventional pretreatment of open intake). The maximum design recovery rate of the PV is just 40% for general feed conditions (TDS 35000 mg/L, temperature 20 °C, and pH 8.2) when higher flux membrane elements are located in the front position. This maximum design recovery rate is because of exceeding the recovery rate limit or maximum design

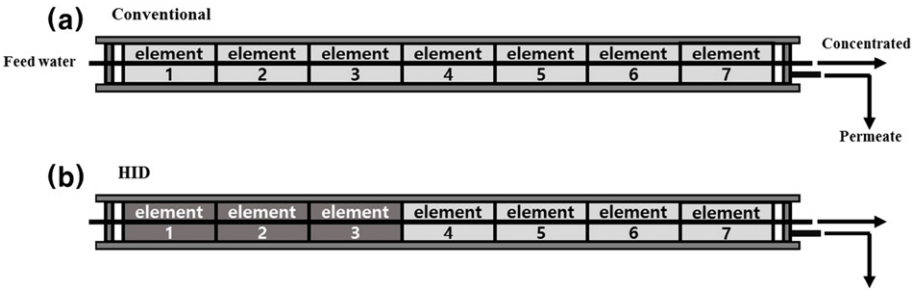

Fig. 1. Schematic diagram of the single-pass SWRO vessel (a) conventional design and (b) HID.

Table 3
Target location feed quality data.

Location	Feed TDS (mg/L)	Temperature (°C)	pH	Boron concentration (mg/L)	Reference
Case 1	40,200	28	8.1	5	[38]
Case 2	33,000	32	7.9	4.2	[41]
Case 3	37,100	20	7.5	5.5	[19]

flux by >40% of the recovery rate. However, when higher flux membrane elements are located in the tail position, the maximum design recovery rate is 50%. Maximum design recovery rates could be determined by feed water quality (e.g., TDS and temperature). Nevertheless, when a higher flux membrane is located in the tail position, the design recovery rate range is relatively large. The best location for high-flux membranes is in the tail position to design a high recovery rate.

The advantage of an ISD is the elimination of unbalanced flux distribution problems. An unbalanced flux distribution causes a relatively high flux in the front position elements; thus, their flux easily exceeds the flux limit and recovery rate that may be the initial point of fouling. HID 6 has an unbalanced flux distribution at 30% recovery and is considerably more severe than HID 4. The HID 4 permeate flow rate of the first front position element (13.25 m^3/d) is 2.11 times higher than that positioned on the last tail (6.27 m^3/d). HID 6 permeate flow rates of the first front position element (19.1 m^3/d) are 4.26 times higher than those positioned on the last tail (4.48 m^3/d). HID 4 permeate flow rates of the first front position element (24.18 m^3/d) at 50% recovery are 3.04 times higher than those positioned on the last tail (7.95 m^3/d). HID 6 permeate flow rates of the first front position element (34.1 m^3/d) are 5.76 times higher than those positioned on the last tail (5.91 m^3/d). Broad design range and low fouling result when higher flux membranes are located on tail position elements instead of front position elements.

3.3. Case study

3.3.1. Optimal recovery rate

Fig. 5 shows the optimal recovery rate with SEC at Case 1, Case 2 and Case 3. In the Case 1, the XHR, HRLE, HID 1, and HID 2 PV designs can operate at the optimal recovery rate (45%). However, ULE, HID 3, HID 4, HID 5, and HID 6 cannot operate at this level owing to the design guidelines for maximum element recovery rate and recommended element permeate flow which were suggested by the membrane manufacturer. Average flux is 13.46, 15.38, and 17.3 LMH at 35%, 40%, and 45% recovery rates, respectively. The highest SEC value is 6.6 kWh/m^3 at the XHR design 30% recovery rate, and the lowest SEC value is 5.19 kWh/m^3 at the ULE design 40% recovery rate.

Also, the designs which were operated on optimal recovery rate (50%) were XHR, HID1, and HID 2 in the Case 2. The highest SEC value is 5.44 kWh/m^3 at the XHR design 30% recovery rate, and the lowest SEC value is 4.25 kWh/m^3 at the ULE design 40% recovery rate. Allowable recovery rates of XHR and HID 3 are higher than those of Case 1. In the Case 3, optimal recovery rates were changed by each PV design. The optimal recovery rates were 50%, HRLE, HID1, HID 2, and HID 4, and 45% XHR. The highest SEC value is 6.42 kWh/m^3 at the XHR 30% design recovery rate, and the lowest SEC value is 4.86 kWh/m^3 at the ULE design 40% recovery rate. Front design (higher flux membrane located on front position) showed high performance on the result Section 3.2. However, Fig. 5 indicated that recovery rate ranges of these front design which were HID 3, HID 5 and HID 6 was limited on high temperature feed conditions (Case 1 and Case 2).

3.3.2. TDS and boron rejection

Fig. 6 shows the permeate TDS and boron concentration by comparing SEC at each possible recovery rate. Although XHR, HRLE, HID 1, HID 3, and HID 5 can satisfy the TDS standard concentration over an entire range of recovery rates on Case 1 feed condition, the ULE PV design cannot. Moreover, the HID 4 and HID 6 designs can operate at only 45% (permeate TDS 394.45 mg/L) and 35% (permeate TDS 389.39 mg/L). The HID 2 design can operate from 40% (permeate TDS 384.79 mg/L) to 50% (permeate TDS 360.72 mg/L). While XHR and HID 3 can satisfy the boron standard concentration for water products on an entire range of recovery rates, ULE, HID 2, HID 4, HID 5, and HID 6 PV designs cannot. Furthermore, the HID 1 design can operate except at 30% (permeate boron concentration 1.00 mg/L), and the HRLE design can operate from 40% (permeate boron concentration 0.98 mg/L) to 45% (permeate boron concentration 0.95 mg/L). The limiting factor is the permeate boron concentration for an SWRO single-pass plant in the Case 1. Optimal PV design is the HRLE at 45% recovery rate. The lowest SEC is 5.52 kWh/m^3 without ERD.

Similar results were shown on Case 2. This TDS value was relatively less than that of Case 1, but temperature was high (32 °C). However, the optimal design results by permeate TDS equal to Case 1, even if TDS value was totally different.

The operating conditions of the HID 4 and HID 6 designs are only 45% (permeate TDS 396.71 mg/L) and 35% (permeate TDS 392.25 mg/L), respectively. The HID 2 design can operate from 40% (permeate TDS 387.22 mg/L) to 50% (permeate TDS 362.52 mg/L). Also, Case 2 design limiting factor for PV optimization was permeate boron concentration. Optimal PV design is HID 1 at 50% recovery rate. The SEC is 4.30 kWh/m^3.

In Case 3, overall PV design can operate on all recovery rates ranges. TDS values are not a limiting factor in the single-pass SWRO process owing to the low temperature of the feed water. XHR, HRLE, HID 1, and HID 3 have no limiting operating recovery rates for boron standards. Moreover, HID 4 and HID 6 designs can operate at 40% (permeate boron concentration 0.99 mg/L) and 50% (permeate boron concentration 0.98 mg/L). The HID 2 design can operate from 40% (permeate boron concentration 0.98 mg/L) to 50% (permeate boron concentration 1.02 mg/L) and the HID 5 design can operate, except at 30% (permeate boron concentration 1.00 mg/L). So, optimal PV design is HID 1 at 50% recovery rate. The SEC is 4.30 kWh/m^3 without ERD under an optimal pressure vessel condition.

3.4. Analysis of case study

Case 1 and Case 2's TDS concentrations are completely different (40,200 mg/L and 33,000 mg/L), but optimal PV design is the same for a permeate 400 mg/L TDS concentration. Optimal PV design for TDS is significantly related to the temperature rather than the concentration of the feed. However, a high TDS value in Case 1 causes high osmotic pressure at the tail of the PV and increases the operational pressure in all vessels. Although the optimal PV design in Case 2 is the same as the Case 1n case for permeate TDS concentration, SEC is apparently different owing to TDS concentration.

Maximum recovery rate of a PV is affected by feed TDS, temperature, and front position membrane type. Low TDS, high-flux membrane, and high temperature in Case 2 cause high permeate flux of membrane elements on the front position of HID 5, HID 6, and ULE. Maximum recovery rates of membrane elements in the front position are limited as seen for HID 6 in Fig. 4. Therefore, they can operate, even in the smallest range. In contrast, maximum recovery rates for Case 3 are determined only by the recovery rate limitation of front position membrane type owing to the low temperature and general TDS values. Increased

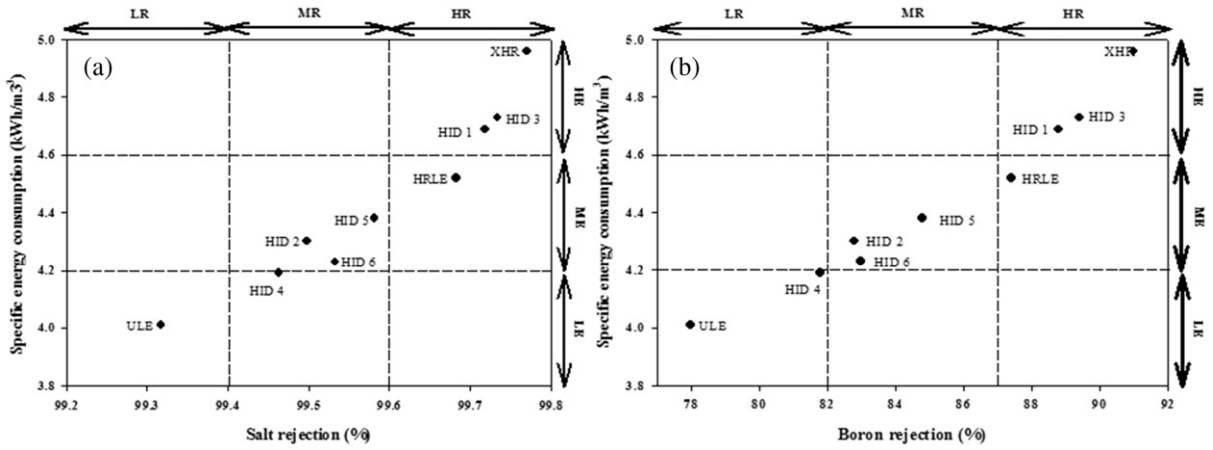

Fig. 2. Comparison of rejection rates for (a) TDS and (b) boron with SEC on a single-pass PV without an ERD. The LR, MR and HR are abbreviation of low rejection, medium rejection and high rejection respectively for simply visualizing rejection rate level. Also, HE, ME and LE indicate high energy consumption, medium energy consumption and low energy consumption.

temperature in feed increases flux and TDS concentration in permeate. Thus, in Case 1 and Case 2, portions of the HID PVs cannot be applied to control TDS values below 400 mg/L.

In the single-train design, the most important parameter is boron concentration. The range of HID is limited beyond that for controlling the TDS concentration to keep the boron concentration below 1 mg/L. The boron concentration in permeate is more sensitive to feed temperature as it is similar in all three cases. Therefore, SW30XHR-400i is necessary for boron control at 32 °C (Case 2), which is the highest temperature in this study, despite a lower boron concentration than in Case 1. HRLE in the Case 1 could satisfy 1 mg/L of the boron concentration. In contrast, SW30ULE-400i in the Case 3 could be applied to HID in the PV owing to the low temperature. These results indicate that a combination of high-flux membranes in HID is thoroughly dependent on feed temperature to control TDS or boron concentration.

Table 4 shows the optimal HID in each respective case and the importance of HID. The HRLE (45%) design was selected as the optimal PV design for the feed quality in Case 1 because the high 28 °C temperature blocks the application of the SW30ULE-400i in HID. The highest flux membrane used at this temperature is SW30HRLE-400i.

When the HID technique is not considered, the XHR (50%) and HRLE (50%) designs were selected in Case 2 and the Case 3, respectively. In contrast, the optimal PV designs when the HID technique is applied are the HID 1 (50%) and HID 4 (50%) designs in Case 2 and the Case 3.

SEC of HID 1 (50%) and XHR (50%) are 4.74 kWh/m^3 and 4.57 kWh/m^3, respectively, and SEC of HID 4 (50%) and HRLE (50%) are 4.99 kWh/m^3 and 5.40 kWh/m^3, respectively. When applying the HID technique, 0.17 and 0.41 kWh/m^3 are reduced with same recovery rate and same feed qualities. Consequently, the HID technique can optimize PV design more specifically for various feed qualities.

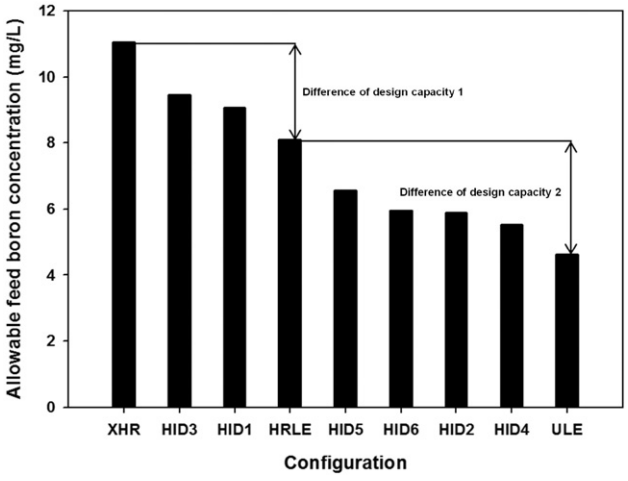

Fig. 3. The design boron concentration range in RO configuration (20 °C, salt 35,000 ppm, and 45% recovery rate).

3.5. Critical design factors of HID

Many design factors influence HID design. The salt rejection rates of HID are determined by temperature and recovery rate. Temperature causes changes in salt flux on the membrane. Average flux of PV is determined by recovery rates and thus the total rejection also changes. It has been mentioned that permeate boron concentration is a vital criterion for HID design according to previous results. Therefore, the allowable boron concentration of feed water was investigated to determine the critical design factor for HID. Fig. 7 shows the allowable feed boron concentration for each PV design. Each membrane type has a different change in allowable feed boron concentration depending on temperature and recovery rate. HID results indicate that boron rejection is significantly affected by membrane type. HID 2, HID 4, HID 5, and HID 6 used a SW30ULE-400i membrane. However, HID 1 and HID 3 did not use the SW30ULE-400i membrane.

The ULE design does not significantly change with temperature and recovery rate. HID 2, HID 4, HID 5, and HID 6 also follow their composition membrane types, which are ULE membranes. Allowable feed boron concentration changes with temperature and recovery rate in the same membrane configuration. Temperature has a greater difference than the recovery rates of both the conventional design and HID between these two design factors. The highest allowable feed boron concentration of XHR decreases by 19.74% from 11.51 mg/L (20 °C) to 6.82 mg/L (30 °C) at a 50% recovery rate by temperature change but by 39.20% from 11.51 mg/L (50%) to 9.24 mg/L (30%) at a temperature of 30 °C by recovery rate change. XHR results show that temperature has more influence on allowable boron feed concentration than recovery rate.

HID also has the same results with conventional design. The highest allowable feed boron concentration of HID 3 decreased by 19.32% from 9.89 mg/L (50% recovery rate) to 7.98 mg/L (30% recovery rate) at a temperature of 20 °C and by 38.46% from 9.89 mg/L (20 °C) to 4.91 mg/L (30 °C) at 50% recovery rate by temperature change. High temperatures narrow the range of allowable feed boron concentration.

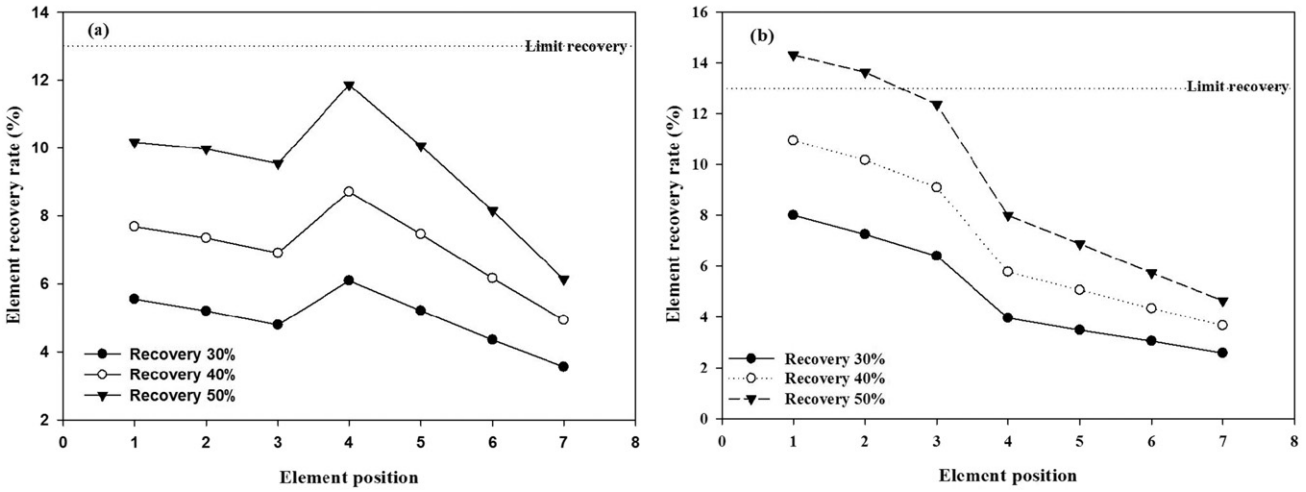

Fig. 4. Comparison of element recovery rate of (a) HID 4 and (b) HID 6 as a function of recovery rate.

However, low temperature and high recovery rate expand the range of allowable feed boron concentration. This indicates that there are no significant performance differences among the HID and conventional designs at high temperature ranges. Accordingly, HID could be used more effectively at low temperature ranges, because results Section 3.1 already shows that the advantage of HID redeem the difference of design capacity to satisfy the required quality by the relationship between rejection rate and SEC. If the differences of design capacity are narrowed, HID design will show less benefit of tailoring the process performance with a marginal difference comparing to the conventional design.

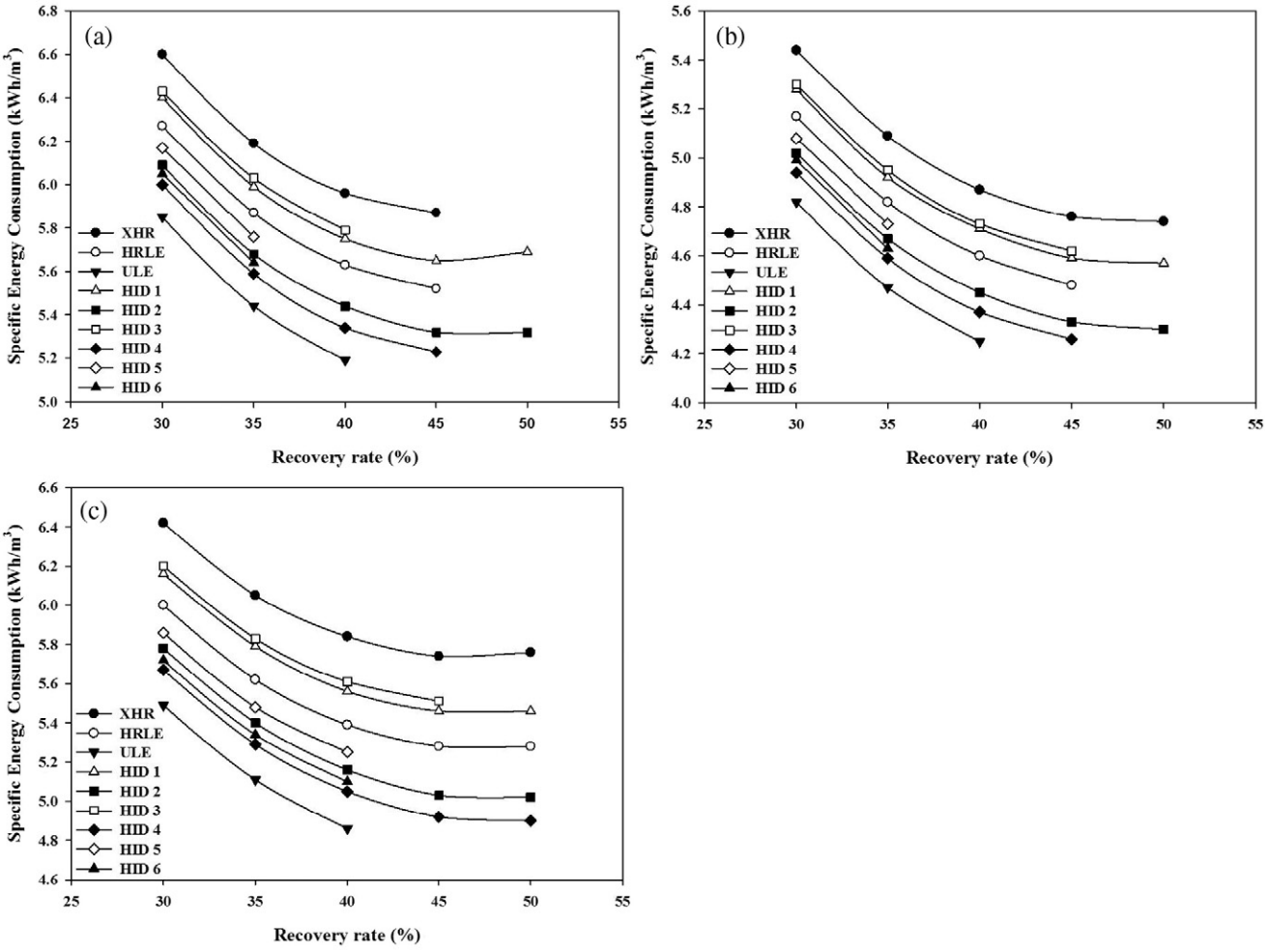

Fig. 5. Optimal recovery rate of each PV design by SEC at (a) Case 1, (b) Case 2 and (c) Case 3.

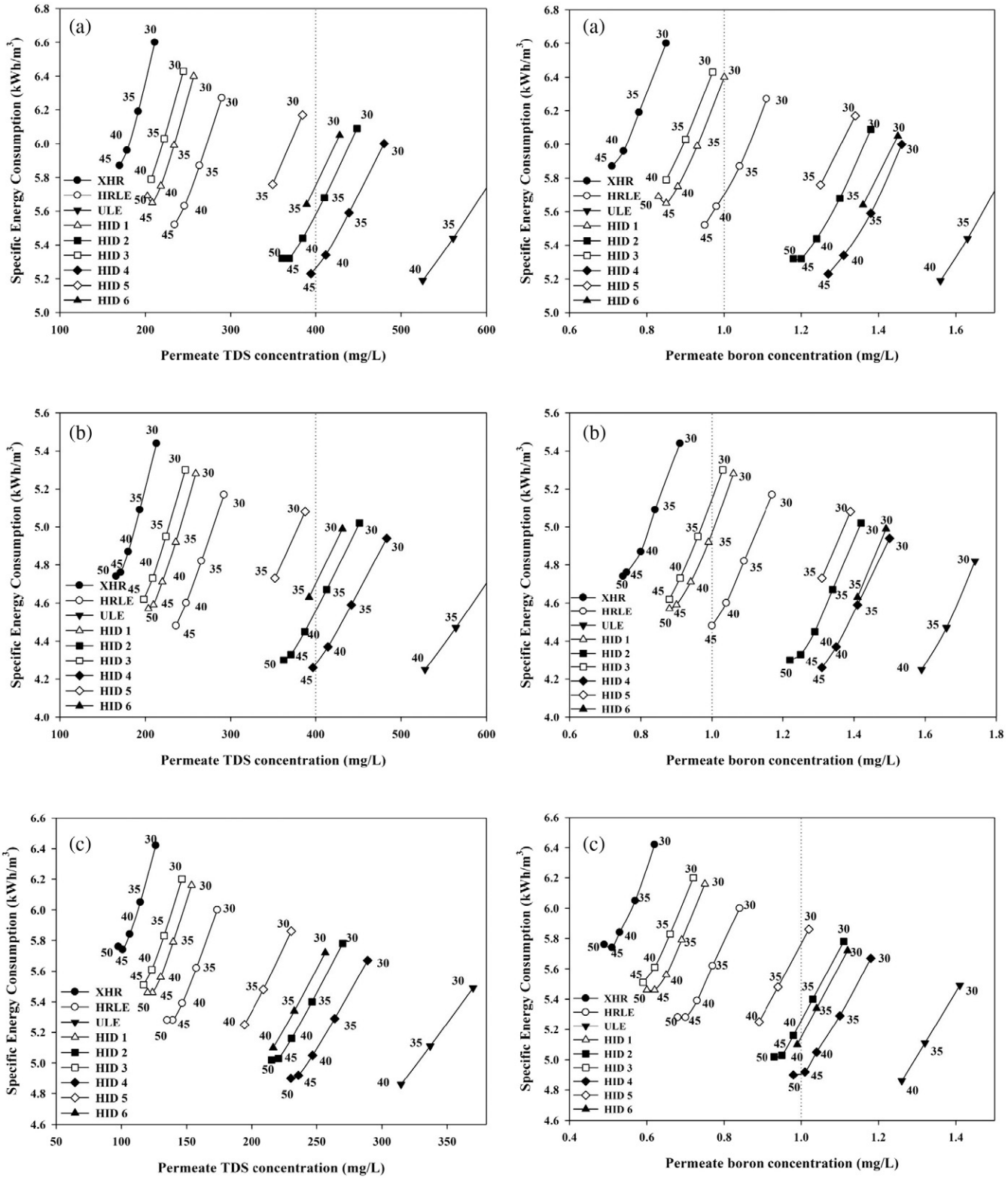

Fig. 6. The performance of each PV design by permeate boron concentration, TDS concentration, SEC and characteristic recovery rates for (a) Case 1, (b) Case 2 and (c) Case 3 without ERD. (Numbers at each symbol indicate the recovery rates).

4. Conclusions

This work reports the optimal combination of RO membranes in PVs with various feed qualities using three distinguished commercial membranes: high-rejection, standard, and high-flux. This study investigated the module configuration and determined the effect of element position in PV. The tail position showed more effect on water quality but the front membrane configuration in the PV influenced more impact on flux. This means the position of high-flux membranes in the PV may determine permeate quality and SEC. Therefore, module configuration can be designed to control water quality level or energy reduction depending on feed water concentration and temperature.

Table 4
Membrane configuration of conventional and HID PV designs.

Case location	Optimal PV design without HID (operating recovery)	Optimal PV design with HID (operating recovery)	Reduction of SEC (kWh/m^3)
Case 1	HRLE (45%)	HRLE (45%)	–
Case 2	XHR (50%)	HID 1 (50%)	0.17
Case 3	HRLE (50%)	HID 4 (50%)	0.41

HID can partially supplement the range designed by a single RO membrane type. RO membrane types and positions in the PV affected the performance in this study. Optimal design of RO membrane configuration in the PV is greatly changed depending on the design parameters, particularly temperature. This is considered important in single-pass train design where the control of boron concentration is more sensitive to the feed temperature than other parameters. The use of high-flux membrane limits permeate quality by feed temperature. However, HID could be used to optimize PV design in more detail with various feed qualities.

Acknowledgements

This research was supported by a grant (16IFIP-B089908-03) from the Plant Research Program funded by the Ministry of Land Infrastructure and Transport of the Korean government.

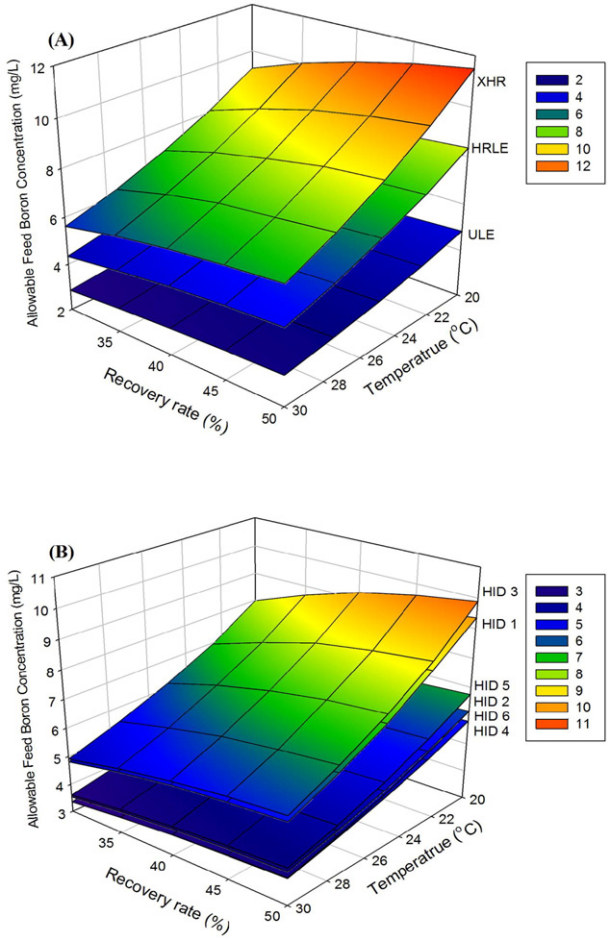

Fig. 7. Comparison of allowable feed boron concentration in design (A) conventional and (B) HID.

References

[1] L.F. Greenlee, D.F. Lawler, B.D. Freeman, B. Marrot, P. Moulin, Reverse osmosis desalination: water sources, technology, and today's challenges, Water Res. 43 (2009) 2317–2348.
[2] B. Peñate, L. García-Rodríguez, Current trends and future prospects in the design of seawater reverse osmosis desalination technology, Desalination 284 (2012) 1–8.
[3] R. Semiat, Energy issues in desalination processes, Environ. Sci. Technol. 42 (2008) 8193–8201.
[4] W.A.P.M. Elimelech, The future of seawater desalination energy, technology, and the environment, Science 333 (2011) 712–717.
[5] R.J. Petersen, J.E. Cadotte, R.E. Larson, E.E. Erickson, A new thin-film composite seawater reverse osmosis membrane, Desalination 32 (1980) 25–31.
[6] R.J. Petersen, Composite reverse osmosis and nanofiltration membranes, J. Membr. Sci. 83 (1993) 81–150.
[7] A.F. Ismail, M. Padaki, N. Hilal, T. Matsuura, W.J. Lau, Thin film composite membrane — recent development and future potential, Desalination 356 (2015) 140–148.
[8] R.L. Stover, Seawater reverse osmosis with isobaric energy recovery devices, Desalination 203 (2007) 168–175.
[9] N. Ghaffour, T.M. Missimer, G.L. Amy, Technical review and evaluation of the economics of water desalination: current and future challenges for better water supply sustainability, Desalination 309 (2013) 197–207.
[10] S.-J. Kim, J. Lee, H.-W. Yu, I.S. Kim, Study on mass production of aquaporinZ for biomimetic water purification membrane, Desalin. Water Treat. 51 (2013) 6370–6377.
[11] A. Zhu, P.D. Christofides, Y. Cohen, Minimization of energy consumption for a two-pass membrane desalination: effect of energy recovery, membrane rejection and retentate recycling, J. Membr. Sci. 339 (2009) 126–137.
[12] M. Li, Reducing specific energy consumption in reverse osmosis (RO) water desalination: an analysis from first principles, Desalination 276 (2011) 128–135.
[13] K.H. Mistry, R.K. McGovern, G.P. Thiel, E.K. Summers, S.M. Zubair, J.H. Lienhard V, Entropy generation analysis of desalination technologies, Entropy 13 (2011) (1829–1864).
[14] M. Li, Energy consumption in spiral-wound seawater reverse osmosis at the thermodynamic limit, Ind. Eng. Chem. Res. 53 (2014) 3293–3299.
[15] W.I.P. Organization, Apparatus for Treating Solutions of High Osmotic Strength, Patent Application Number PCT/US2005/006224, 2005.
[16] V.G. Molina, M. Busch, P. Sehn, Cost savings by novel seawater reverse osmosis elements and design concepts, Desalin. Water Treat. 7 (2009) 160–177.
[17] H. Winters, Twenty-years-experience-in-seawater-reverse-osmosis-and-how-chemicals-in-pretreatment-affect-fouling-of-membranes, Desalination 110 (1997) 93–96.
[18] S.-J. Kim, B.S. Oh, H.-W. Yu, L.H. Kim, C.-M. Kim, E.-T. Yang, M.S. Shin, A. Jang, M.H. Hwang, I.S. Kim, Foulant characterization and distribution in spiral wound reverse osmosis membranes from different pressure vessels, Desalination 370 (2015) 44–52.
[19] B. Peñate, L. García-Rodríguez, Reverse osmosis hybrid membrane inter-stage design: a comparative performance assessment, Desalination 281 (2011) 354–363.
[20] F. Vince, F. Marechal, E. Aoustin, P. Bréant, Multi-objective optimization of RO desalination plants, Desalination 222 (2008) 96–118.
[21] Y. Saif, A. Almansoori, Synthesis of reverse osmosis desalination network under boron specifications, Desalination 371 (2015) 26–36.
[22] S. Lin, M. Elimelech, Staged reverse osmosis operation: configurations, energy efficiency, and application potential, Desalination 366 (2015) 9–14.
[23] Y. Lu, Y. Hu, D. Xu, L. Wu, Optimum design of reverse osmosis seawater desalination system considering membrane cleaning and replacing, J. Membr. Sci. 282 (2006) 7–13.
[24] Y. Du, L. Xie, Y. Liu, S. Zhang, Y. Xu, Optimization of reverse osmosis networks with split partial second pass design, Desalination 365 (2015) 365–380.
[25] S.Y. Alnouri, P. Linke, Optimal seawater reverse osmosis network design considering product water boron specifications, Desalination 345 (2014) 112–127.
[26] A. Jiang, L.T. Biegler, J. Wang, W. Cheng, Q. Ding, S. Jiangzhou, Optimal operations for large-scale seawater reverse osmosis networks, J. Membr. Sci. 476 (2015) 508–524.
[27] N. Hilal, G.J. Kim, C. Somerfield, Boron removal from saline water: a comprehensive review, Desalination 273 (2011) 23–35.
[28] E. Güler, C. Kaya, N. Kabay, M. Arda, Boron removal from seawater: state-of-the-art review, Desalination 356 (2015) 85–93.
[29] E. Guler, D. Ozakdag, M. Arda, M. Yuksel, N. Kabay, Effect of temperature on seawater desalination-water quality analyses for desalinated seawater for its use as drinking and irrigation water, Environ. Geochem. Health 32 (2010) 335–339.
[30] WHO, Guidelines for Drinking-water Quality, fourth ed. World Health Organization, 2011 (978 92 4 154815 1).
[31] European Union Council Directive 9883EC, of 3 November 1998 on the Quality of Water Intended for Human Consumption(98/83/EC) 1998.
[32] L. Melnyk, V. Goncharuk, I. Butnyk, E. Tsapiuk, Boron removal from natural and wastewaters using combined sorption/membrane process, Desalination 185 (2005) 147–157.

[33] N. Kabay, İ. Yilmaz, M. Bryjak, M. Yüksel, Removal of boron from aqueous solutions by a hybrid ion exchange–membrane process, Desalination 198 (2006) 158–165.
[34] N. Kabay, I. Yılmaz, S. Yamac, S. Samatya, M. Yuksel, U. Yuksel, M. Arda, M. Sağlam, T. Iwanaga, K. Hirowatari, Removal and recovery of boron from geothermal wastewater by selective ion exchange resins. I. Laboratory tests, React. Funct. Polym. 60 (2004) 163–170.
[35] M.F. Chillón Arias, L. Valero i Bru, D. Prats Rico, P. Varó Galvañ, Approximate cost of the elimination of boron in desalinated water by reverse osmosis and ion exchange resins, Desalination 273 (2011) 421–427.
[36] M.B.J. Redondo, J. De Witte, Boron removal from seawater using FILMTEC™ high rejection SWRO membranes, Desalination 156 (2003) 229–238.
[37] H. Koseoglu, N. Kabay, M. Yüksel, S. Sarp, Ö. Arar, M. Kitis, Boron removal from seawater using high rejection SWRO membranes — impact of pH, feed concentration, pressure, and cross-flow velocity, Desalination 227 (2008) 253–263.
[38] C. Dominguez-Tagle, V.J. Romero-Ternero, A.M. Delgado-Torres, Boron removal efficiency in small seawater reverse osmosis systems, Desalination 265 (2011) 43–48.
[39] B. Andrews, B. Davé, P. López-Serrano, S.-P. Tsai, R. Frank, M. Wilf, E. Koutsakos, Effective scale control for seawater RO operating with high feed water pH and temperature, Desalination 220 (2008) 295–304.
[40] M.J.B. Atkinson, C, Elemental composition of commercial seasalts, J. Aquaric. Aquat. Sci. 8 (1998) 39–43.
[41] J.D.N. Voutchkov, Pilot Testing Alternative Pretreatment Systems for Seawater Desalination in Carlsbad, International Desalination Association, IDAWC/DB09-309, Dubai, UAE, November 7–12, 2009.